Structural Engineering and Mechanics, *Vol. 55, No. 2 (2015) 379-398*
DOI: http://dx.doi.org/10.12989/sem.2015.55.2.379

Redistribution of moments in reinforced high-strength concrete beams with and without confinement

Tiejiong Lou[1], Sergio M.R. Lopes[*1] and Adelino V. Lopes[2]

[1]*CEMUC, Department of Civil Engineering, University of Coimbra, Coimbra 3030-788, Portugal*
[2]*Department of Civil Engineering, University of Coimbra, Coimbra 3030-788, Portugal*

(Received March 1, 2015, Revised April 25, 2015, Accepted June 16, 2015)

Abstract. Confinement is known to have important influence on ductility of high-strength concrete (HSC) members and it may therefore be anticipated that this parameter would also affect notably the moment redistribution in these members. The correctness of this "common-sense knowledge" is examined in the present study. A numerical test is performed on two-span continuous reinforced HSC beams with and without confinement using an experimentally validated nonlinear model. The results show that the effect of confinement on moment redistribution is totally different from that on flexural ductility. The moment redistribution at ultimate limit state is found to be almost independent of the confinement, provided that both the negative and positive plastic hinges have formed at failure. The numerical findings are consistent with tests performed on prototype HSC beams. Several design codes are evaluated. It is demonstrated that the code equations by Eurocode 2 (EC2), British Standards Institution (BSI) and Canadian Standards Association (CSA) can well reflect the effect of confinement on moment redistribution in reinforced HSC beams but the American Concrete Institute (ACI) code cannot.

Keywords: high-strength concrete; confinement; moment redistribution; ductility; continuous beams

1. Introduction

High-strength concrete (HSC) has been widely used in the construction industry owing to its main advantages including great mechanical performance and excellent durability. However, some concern may arise because of the brittleness of HSC, exemplified by a steeper stress-stain curve with a smaller ultimate compressive strain when compared to the stress-strain law of normal-strength concrete (NSC). Over past years, a great quantity of research has been conducted regarding the ductility and plastic rotation of reinforced HSC members (Bai and Au 2013, Bernardo and Lopes 2004, Campione *et al*. 2012, Carmo and Lopes 2008, Cucchiara *et al*. 2012, Galano and Vignoli 2008, Kassoul and Bougara 2010). Previous studies demonstrated that a reinforced HSC member, when appropriately designed, can exhibit favorable ductile behavior which can easily meet the plastic rotation requirement for structural safety.

In continuous concrete members, moment redistribution might take place with the first crack initiation and its evolution may be influenced by some phases such as the formation of plastic

∗Corresponding author, Professor, E-mail: sergio@dec.uc.pt

http://www.techno-press.org/?journal=sem&subpage=8 ISSN: 1225-4568 (Print), 1598-6217 (Online)

hinges at critical sections (Lou *et al*. 2013). It is commonly known that there is a close link between moment redistribution and flexural ductility. While the ductile behavior of HSC members has been well examined, limited works have so far been carried out to evaluate the moment redistribution in such members (Carmo and Lopes 2008, Lou *et al*. 2014a, b). The authors have recently conducted a numerical investigation into redistribution of moments in two-span continuous reinforced NSC and HSC beams (Lou *et al*. 2014b). The study showed that HSC tends to mobilize higher moment redistribution than NSC except at a low steel ratio. An explanation for this phenomenon is as follows (Lou *et al*. 2014b): Moment redistribution is heavily dependent on the formation of plastic hinges in the critical regions. It has been shown that both the positive and negative plastic hinges would be developed in a HSC beam with a steel ratio up to a very high level. On the other hand, in a NSC beam with a high steel ratio, only the negative plastic hinge at the intermediate support formed whereas the positive plastic hinges over the span critical regions did not appear. As a result, a HSC beam would redistribute more than a NSC beam.

Apart from the concrete strength, there are many other parameters that may affect notably the ductility and moment redistribution in concrete members (Kodur and Campbell 1999, Lou *et al*. 2014c). Of these parameters, the transverse reinforcement or the resulting confinement has been recognized as an important parameter (Sheikh *et al*. 2013). Extensive works have been done to study the effect of confinement on the ductile behavior of NSC and HSC members (Ho *et al*. 2010, Hwang and Yun 2004, Kwan *et al*. 2004). Adding confinement to concrete was found to be very effective in improving flexural ductility. It may be expected that the moment redistribution capacity in continuous concrete beams could also be effectively enhanced by adding confinement since improved ductility is beneficial to redistribute moments. This statement, which seems to be "common-sense knowledge", has been supported by previous works by other investigators (El-Mogy 2011, Kodur and Campbell 1999, Moucessian 1986), where confinement of concrete was reported to have important influence on moment redistribution in reinforced and prestressed concrete members. It is indicated, however, the aforementioned "common-sense knowledge" about the confinement effect on moment redistribution cannot be applied to reinforced HSC continuous beams, as will be discussed in this study.

This paper presents an investigation conducted to identify the moment redistribution behavior of reinforced HSC continuous beams with and without confinement. A finite element model has been developed and its reliability is verified with the results of laboratory tests which were specifically designed for understanding the effect of transverse reinforcement on moment redistribution in HSC beams. The ductility and redistribution of moments in HSC continuous beams are evaluated using the proposed model and considering different degrees of confinement and various steel ratio levels. In addition, several code recommendations for permissible moment redistribution are examined.

2. Method of numerical analysis

A finite element model based on the moment-curvature relationship for nonlinear analysis of reinforced HSC beams has been developed (Lou *et al*. 2014d). The following assumptions/ simplifications are adopted in the analysis: a plane section remains plane after deformations; there is perfect bond between reinforcement and concrete; the geometric nonlinearity is not considered; and the material stress-strain laws are known.

In Eurocode 2 (EC2) (CEN 2004) and Model Code 1990 (CEB-FIP 1990), the following stress-strain law for unconfined concrete in compression is recommended for structural analysis

$$\frac{\sigma_c}{f_{cm}} = \frac{k\eta - \eta^2}{1 + (k-2)\eta} \tag{1}$$

where $\eta=\varepsilon_c/\varepsilon_{c0}$; σ_c and ε_c are the concrete stress and strain, respectively; $k=1.05E_c\varepsilon_{c0}/f_{cm}$; ε_{c0} is the concrete strain at peak stress, and ε_{c0}(‰)$=0.7\, f_{cm}^{0.31}<2.8$; E_c is the modulus of elasticity of concrete (in GPa), and $E_c=22(f_{cm}/10)^{0.3}$; f_{cm} is the mean compressive strength (in MPa), and $f_{cm}+f_{ck}+8$; f_{ck} is the characteristic cylinder compressive strength (in MPa). Eq. (1) is valid when the concrete strain is not greater than the ultimate compressive strain ε_u, which for HSC may be calculated from

$$\varepsilon_u(‰) = 2.8 + 27[(98 - f_{cm})/100]^4 \tag{2}$$

For confined concrete in compression, the constitutive law recommended in Model Code 1990 (CEB-FIP 1990) is simpler and more practical than that of Model Code 2010 (FIB 2012). It is a modification of the model for unconfined concrete by changing the value of several parameters, as shown in Fig. 1 which represents the constitutive laws of confined and unconfined concrete in compression. In the absence of more precise data, the following relationships between the parameters for confined and unconfined concrete may be used

$$f_{cm}^* = f_{cm}(1.0 + 2.5C_c) \quad \text{for} \quad \sigma_2 < 0.05 f_{cm} \tag{3a}$$

$$f_{cm}^* = f_{cm}(1.125 + 1.25C_c) \quad \text{for} \quad \sigma_2 > 0.05 f_{cm} \tag{3b}$$

$$\varepsilon_{c0}^* = \varepsilon_{c0}(f_{cm}^* / f_{cm})^2 \tag{4}$$

$$\varepsilon_u^* = \varepsilon_u + 0.1C_c \tag{5}$$

where f_{cm}^*, ε_{c0}^*, and ε_u^* are the confined concrete strength, strain at confined peak stress and confined ultimate strain, respectively; C_c is the confining coefficient and $C_c=\alpha\omega_w$; ω_w is the volumetric mechanical ratio of confining steel; α is the effectiveness of confinement, equal to $\alpha_n\alpha_s$, where α_n depends on the arrangement of stirrups in the cross section and α_s depends on the spacing of stirrups; and σ_2 is the effective lateral compression stress due to confinement. Using this model, the confinement condition can be defined in terms of the value of the confining coefficient C_c. $C_c=0$ indicating unconfined concrete, while $C_c>0$ indicating confined concrete. The larger the value of C_c, the higher would be the degree of the confinement.

The stress-strain behavior for concrete in tension is simulated using a bilinear elastic-softening law, where the concrete tensile strength may be quantified in terms of Eurocode 2 (CEN 2004). The stress-strain behavior for reinforcing steel in both tension and compression is simulated using a bilinear elastic-hardening law, where the modulus for the strain-hardening portion is assumed to be 1.5% of the modulus of elasticity.

The moment-curvature relationship is generated through cross-sectional analysis by satisfying strain compatibility and force equilibrium conditions. The layered technique is applied to consider different material properties across the depth of the section. In order to construct the complete moment-curvature curve of a section, the curvature is increased monotonically with a small step starting from zero. When the concrete reaches its ultimate compressive strain or the reinforcement

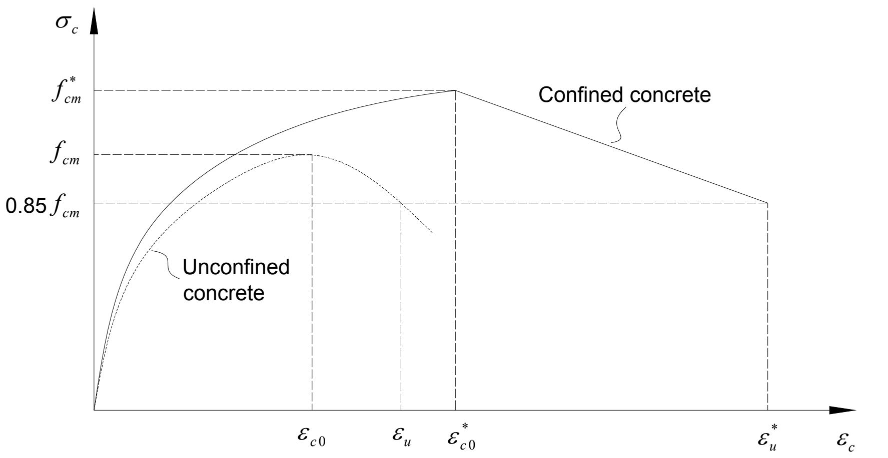

Fig. 1 Stress-strain curves for confined and unconfined concrete in compression

gets to its ultimate strength, failure of the section takes place. The finite element method is formulated on the basis of the Timoshenko beam theory taking into account the transverse shear deformation. The beam is idealized as two-node beam elements. Each node has two degrees of freedom, namely, transverse displacement and rotation. The transverse displacement and rotation within each element are approximated by linear interpolation. The element equilibrium equations are determined by applying the principle of virtual work. The stiffness matrix consists of two components, namely, the bending stiffness matrix and the shear stiffness matrix. To avoid the shear locking problem, the shear stiffness matrix is evaluated by using one-point Gauss quadrature instead of two-point Gauss quadrature. The structure equilibrium equations are assembled in the global coordinate system from the contributions of all elements. An incremental method combined with the Newton-Raphson iterative scheme is employed to solve the nonlinear equilibrium equations. During the solution process, when one of the elements reaches its ultimate curvature capacity, the beam fails and the analysis is therefore finished. The proposed model is capable of performing the material nonlinear analysis of reinforced HSC continuous beams with and without confinement throughout the loading range up to failure.

3. Tests and comparison to numerical predictions

In an experimental program performed in Coimbra (Carmo 2004), six two-span continuous HSC beams were tested up to failure in order to examine the effect of concrete confinement on the redistribution of moments. These beams were V2-0.5-4, V2-0.8-4, V2-1.6-4, V2-0.5-5, V2-0.8-5 and V2-1.6-5. For the first three beams the tensile steel area over the center support region was 804 mm^2, while for the last three beams it was 1030 mm^2. Three configurations of transverse reinforcement over the center support region were chosen so as to produce different degrees of concrete confinement: 6 mm stirrups with spacing of 100 mm for V2-0.5-4 and V2-0.5-5, 8 mm stirrups with spacing of 100 mm for V2-0.8-4 and V2-0.8-5, and 8 mm stirrups with spacing of 50 mm for V2-1.6-4 and V2-1.6-5. The structure, section and reinforcement details are shown in Fig.

2(a), where A_{s1} and A_{s2} are the tensile steel areas at positive and negative moment regions, respectively; and A_{s3} and A_{s4} are compressive steel areas at positive and negative moment regions, respectively. The yield strength and ultimate strength of steel were 569 and 669 MPa, respectively. The beams were made of HSC having an average cylinder compressive strength of 71 MPa at age of 28 days.

The load was applied by a hydraulic jack. The load increment varied between 10 and 25 kN, depending on the stage of the test. The support reactions were measured by load cells placed under the supports. The values of the support reactions enable the redistribution of moments along the span to be determined at any stage of the test. The readings of the support reactions must be as accurate as possible, so experiments were carefully planned to ensure the beam undisturbed on its supports throughout the testing process. More details about the experimental program can be seen elsewhere (Carmo 2004).

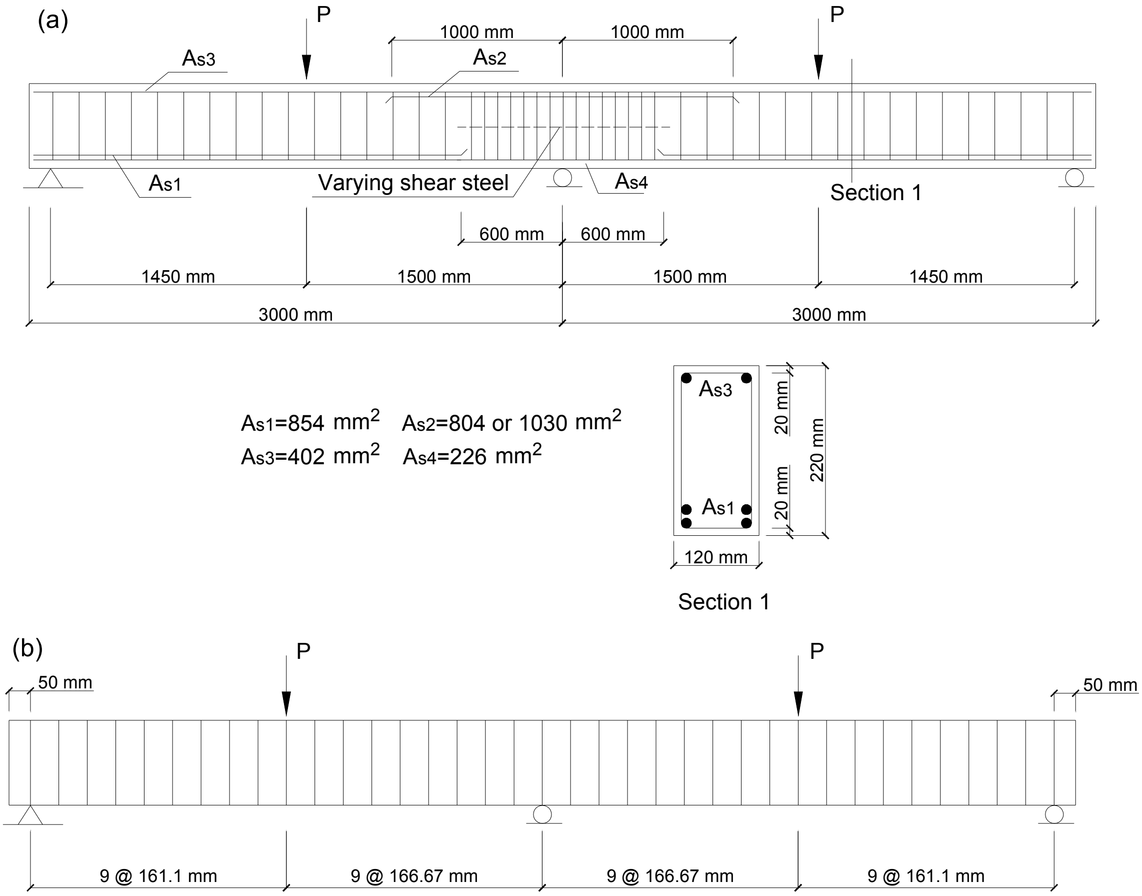

Fig. 2 Experimental beams and the finite element model. (a) details of experimental beams; (b) finite element model

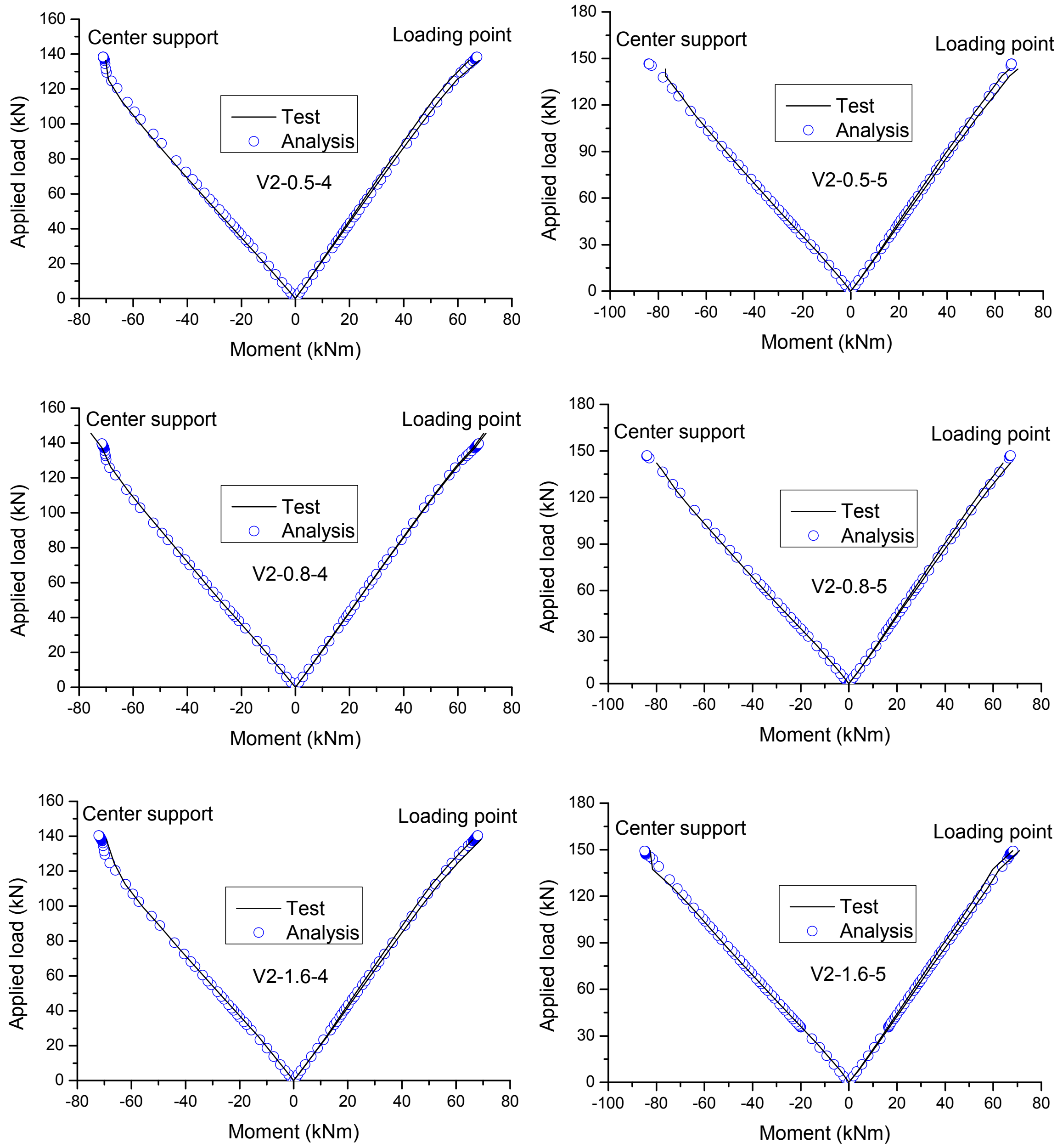

Fig. 3 Comparison between experimentally obtained load-moment curves and numerical predictions

The finite element model of the beams is shown in Fig. 2(b). The analysis consists of two steps: load control analysis of the beams under self-weight load; and displacement control analysis of the beams under increasing applied loads up to failure. Fig. 3 shows the load-moment relationship obtained from the tests as well as the predictions by the proposed numerical analysis. Because there is a slight disparity between the readings of the left and right support reactions, the

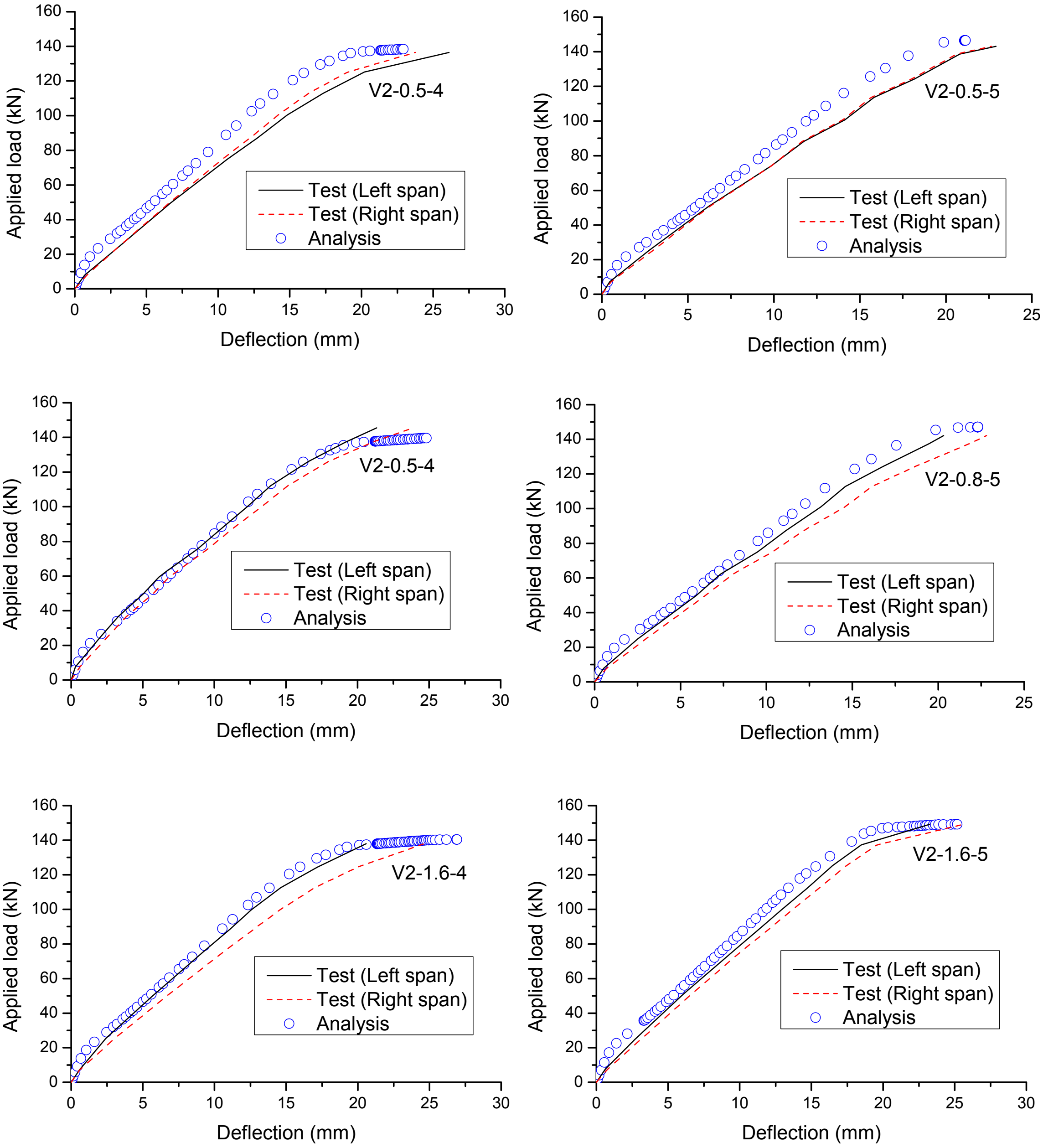

Fig. 4 Comparison between experimentally obtained load-deflection curves and numerical predictions

experimentally obtained moments at two span critical sections (loading points) resulting from the support reactions are slightly different. According to experimental observations, the concrete confinement has practically no effect on moment redistribution in the beams. Beams V2-0.5-4, V2-0.8-4 and V2-1.6-4, where the transverse reinforcement is the only variable, exhibited very

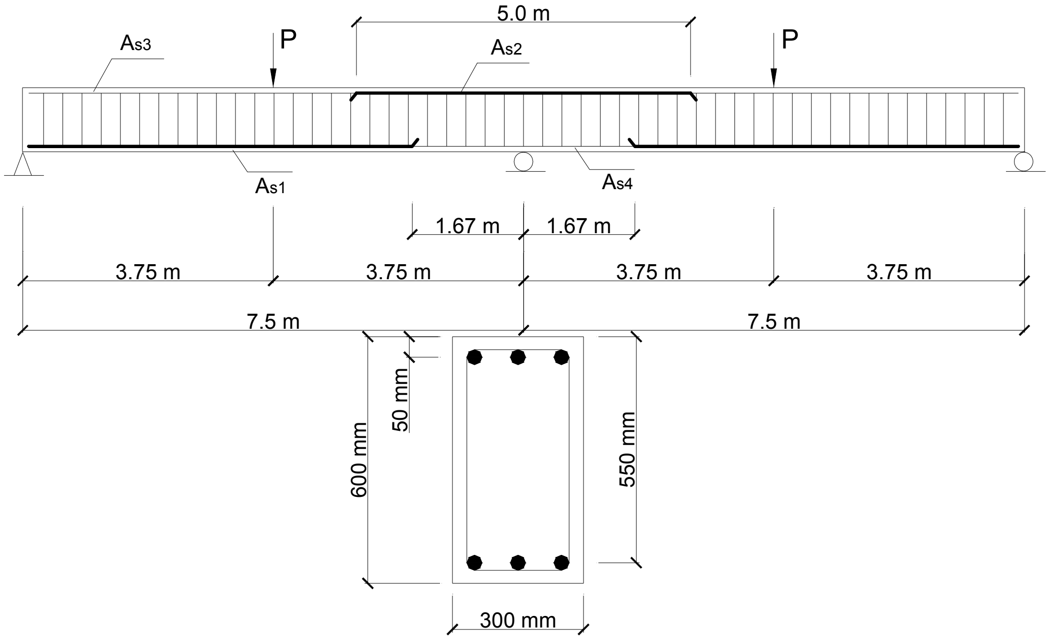

Fig. 5 Details of reference beam for numerical investigation

similar moment evolution behavior up to failure, and so were Beams V2-0.5-5, V2-0.8-5 and V2-1.6-5. The experimental observations of the null effect of concrete confinement on moment redistribution, however, contradict initial expectations, as the provision of confinement is supposed to improve obviously the moment redistribution behavior as a result of enhancing flexural ductility. To examine the correctness of the experimental observations and to further understand the influence of confinement on moment redistribution in HSC beams, an extensive numerical investigation is carried out using the afore-described nonlinear model.

It can be seen in Fig. 3 that the proposed nonlinear analysis reproduces the experimental results regarding the load-moment response with excellent agreement. A comparison between computational and experimental results with regard to the load-deflection curves at loading points is illustrated in Fig. 4. Although the predicted behavior is generally shown to be a bit stiffer than the tests (this may be attributed to the neglect of relative slip between steel and concrete as assumed in the numerical model), favorable agreement can also be observed throughout the whole loading history up to failure.

4. Numerical Investigation

4.1 Beam details

A reinforced HSC rectangular beam continuous over two equal spans to which two center-point loads are symmetrically applied at midspan, as shown in Fig. 5, is used as a reference beam for the numerical investigation. The cylinder compressive strength f_{ck} for HSC is taken as 90 MPa. The

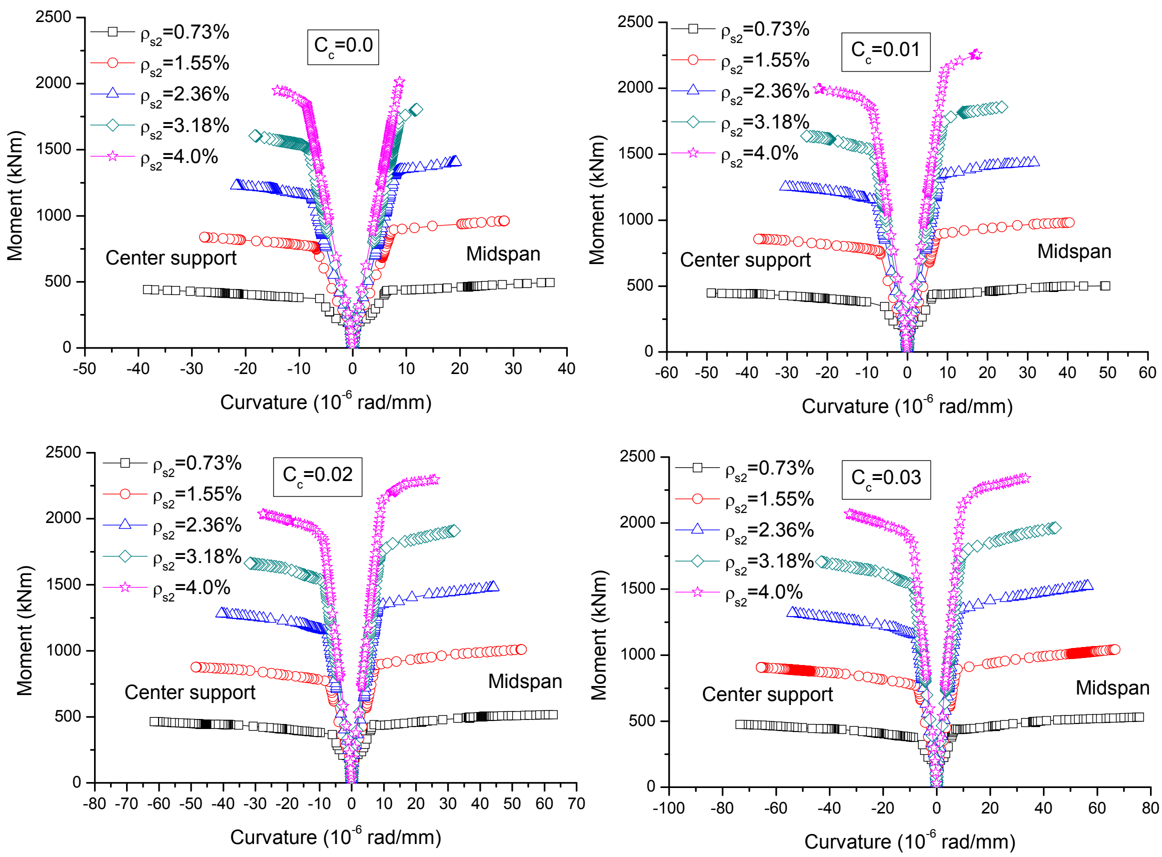

Fig. 6 Moment-curvature curves for the beams having various steel ratios and confinement conditions

area of tensile steel over the negative moment region A_{s2} varies between 1200 and 6600 mm^2, while the ratio A_{s2}/A_{s1} or ρ_{s2}/ρ_{s1} is fixed at 0.8, where ρ_{s1} and ρ_{s2} are the tensile steel ratios at the positive and negative moment regions, respectively. For the compressive steel, $A_{s3}=A_{s4}=600$ mm^2. The yield strength and elastic modulus of steel are taken as 530 MPa and 200 GPa, respectively. Four confinement conditions are considered, namely, $C_c=0$, 0.01, 0.02 and 0.03. Assume that the effective lateral compression stress σ_2 is lower than 4.9 MPa, i.e., $\sigma_2<0.05f_{cm}$. To simplify the analysis, the compressive concrete in the whole beam is assumed to follow the same confinement condition, while the confinement in the concrete tension zone is not considered. In the finite element modeling, the two-span continuous beam is idealized as 36 beam elements having the same length of 416.67 mm.

4.2 Moment-curvature response and flexural ductility

Fig. 6 shows the moment-curvature response for the midspan and center support sections of the beams having various steel ratios and confinement conditions. It should be noted that the moment shown in the graphs was obtained according to the reaction at the end support. At a given element curvature, this moment is a bit higher than the corresponding element moment. The entire response

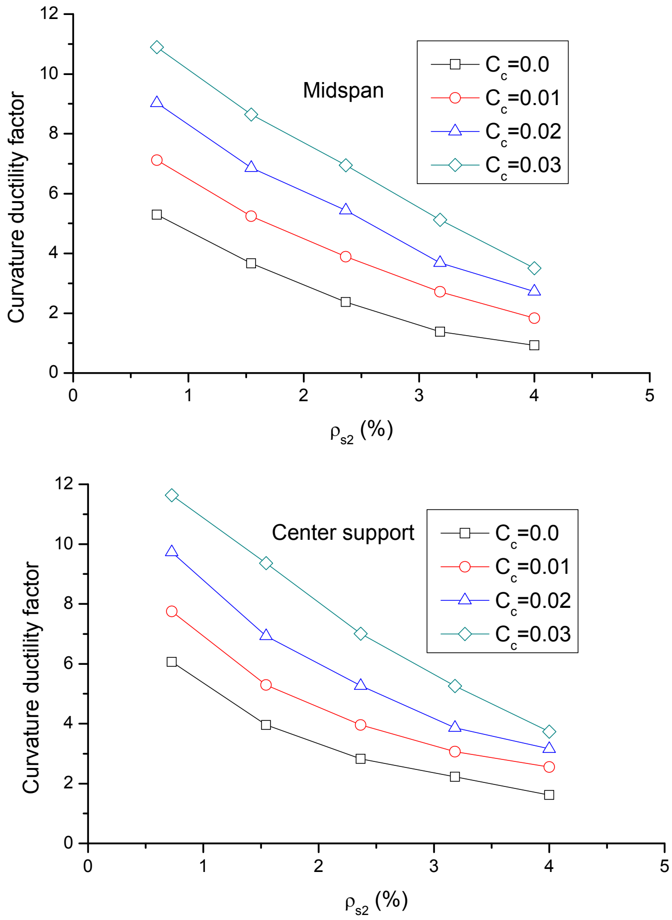

Fig. 7 Variation of curvature ductility with steel ratio for different confinement conditions

is characterized by three stages separated by two points corresponding to concrete cracking and steel yielding, except for the unconfined concrete section containing the highest steel ratio where the steel does not yield at failure. The first stage represents elastic behavior, featured by a slight increase in curvature and a quick increase in moment. In this stage the behavior is primarily controlled by the concrete and, therefore, there is almost an identical response for different levels of steel ratio. After cracking, the steel begins to play an important role in the behavior of the beams. Due to cracking, the stiffness in the second stage is more or less reduced depending on the steel ratios. In this stage a higher steel ratio results in much higher flexural stiffness. In the third stage, due to yielding of steel, the flexural stiffness becomes very weak. The third stage of the moment-curvature behavior reflects the flexural ductility of the beams, which may be measured by the curvature ductility factor μ_ϕ

$$\mu_\phi = \phi_u / \phi_y \tag{6}$$

where ϕ_u and ϕ_y is the curvatures at ultimate and at yielding, respectively.

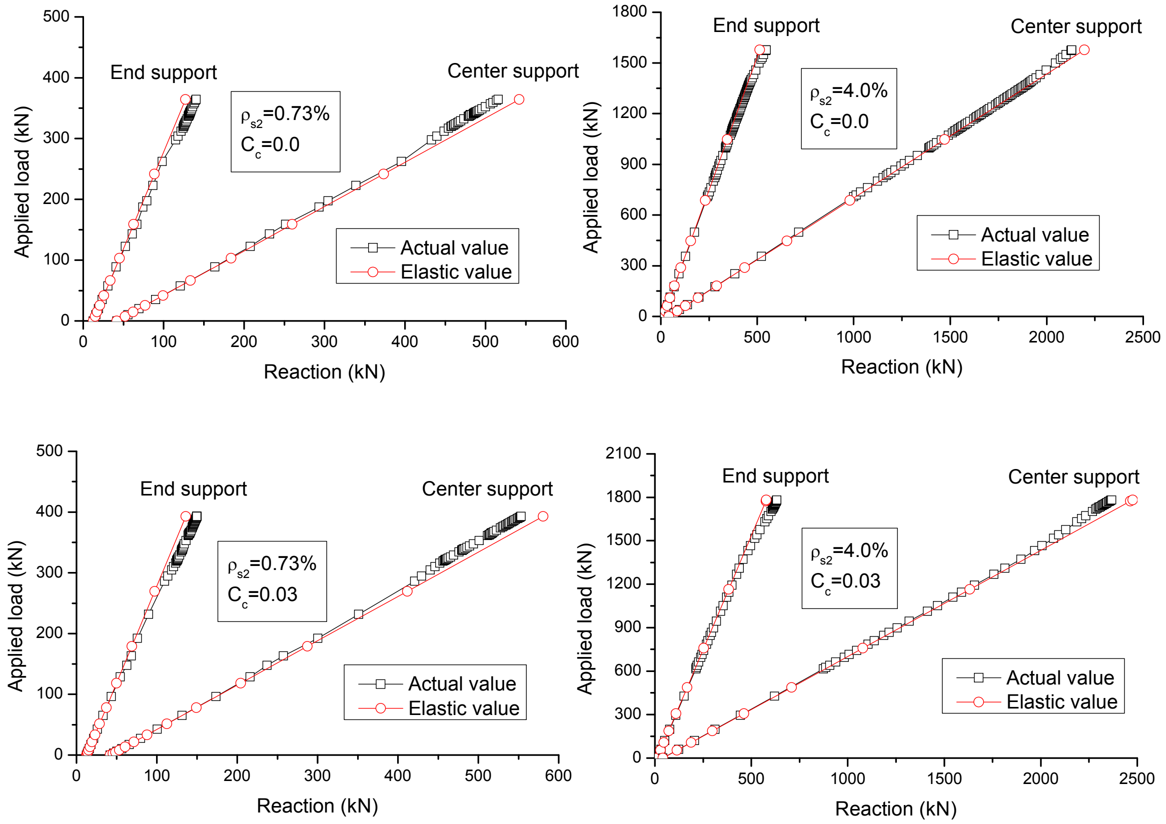

Fig. 8 Development of support reactions for the beams having typical steel ratios and confinement conditions

Fig. 7 shows the variation of μ_ϕ with the steel ratio for different confinement conditions. It is seen that the ductility factor is highly dependent on the steel ratio and confinement. At a given degree of confinement, the ductility quickly decreases as the steel ratio increases. At a given steel ratio, a higher degree of confinement leads to obviously higher ductility, as expected. This phenomenon is particularly notable at a low steel ratio.

4.3 Reaction development and moment diagram

The development of actual and elastic reactions at the end and center supports of the beams having two typical steel ratios as well as two typical confinement conditions is illustrated in Fig. 8. The actual reactions were computed by the nonlinear finite element analysis (FEA), whereas the elastic reactions were calculated from the elastic analysis. It is seen that at early stage of loading (elastic stage), the actual reaction is identical to the elastic one, indicating that moment redistribution does not yet take place in the elastic stage. When cracks appear in concrete, redistribution of moments occurs, leading to a gradual deviation between the actual and elastic reactions. This phenomenon is apparent for a low steel ratio but appears to be not so noticeable for a high steel ratio. When the formation of plastic hinges (in other words, the yielding of tensile

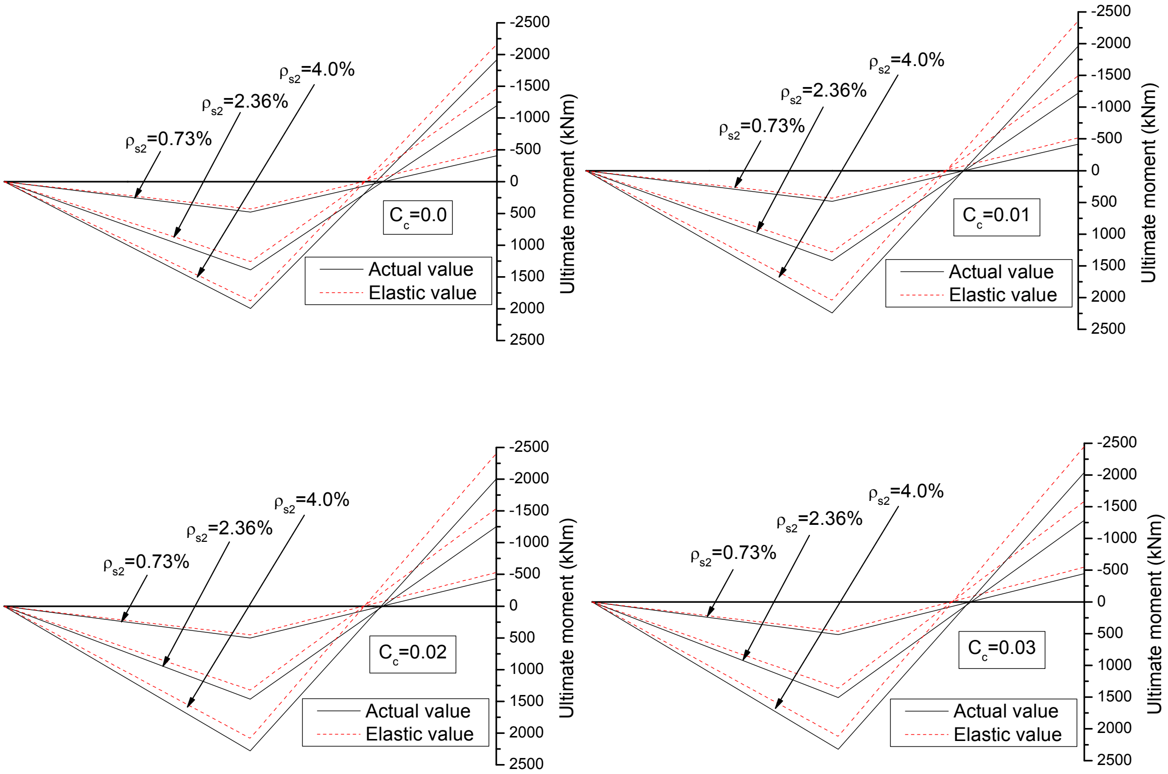

Fig. 9 Moment distribution at ultimate for the beams having various steel ratios and confinement conditions

steel) begins to take place at critical sections of the beams, the increase in deviation between the actual and elastic reactions is accentuated or alleviated, depending on the change in stiffness difference between the critical negative and positive moment sections. Also, it can be observed that at a given steel ratio, the reaction development for unconfined concrete (C_c=0) is very similar to that for confined concrete.

Fig. 9 shows the distribution of actual and elastic applied moments along the span, at the ultimate load, for the beams having different steel ratios and confinement conditions. The applied moment corresponds to the moment caused by the applied load, not including the self-weight moment. These graphs clearly demonstrate how the actual moment distribution differs relative to the distribution obtained from an elastic analysis. It is seen that the actual moment at the midspan region is greater than the corresponding elastic moment, while over the center support region the actual moment is smaller than the corresponding elastic one. This indicates that these beams tend to redistribute moments from the center support region to the midspan region. In addition, it can be observed that the difference between the actual and elastic moments at the center support is always larger than that at midspan.

4.4 Degree of moment redistribution

The redistribution of moments may be measured in terms of the degree of redistribution defined by

$$\beta = (M_e - M) / M_e \tag{7}$$

in which M is the actual moment at an applied load; and M_e is elastic moment corresponding to the applied load.

Fig. 10 shows the evolution of the degree of moment redistribution at the center support and midspan of the beams having various steel ratios and confinement conditions. Before cracking, the actual moment is identical to the elastic one and therefore the value of β is equal to zero. Upon first cracking which takes place at the center support, moments begin to be redistributed from the center support region to the midspan region. As a result, the actual moment at the center support would be smaller than the corresponding elastic moment while it is opposite at midspan, leading to positive redistribution at the center support but negative redistribution at midspan. With continuing increase of the applied load, the value of β quickly increases with a slope depending on the amount of steel: the lower the amount of steel, the steeper would be the slope. This can be explained by the fact that the reduction in flexural stiffness as a result of cracking for a low steel ratio is more significant than that for a high steel ratio. The redistribution then reaches a plateau for the beams

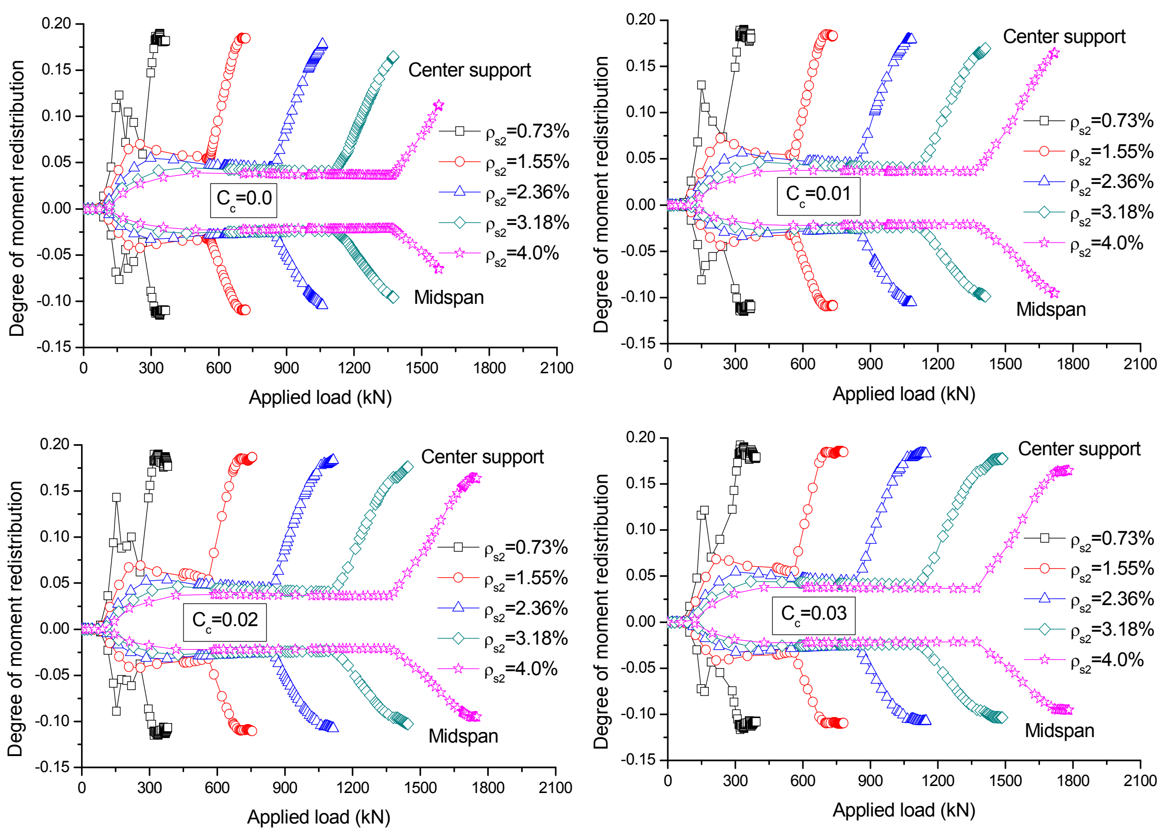

Fig. 10 Development of moment redistribution for the beams having various steel ratios and confinement conditions

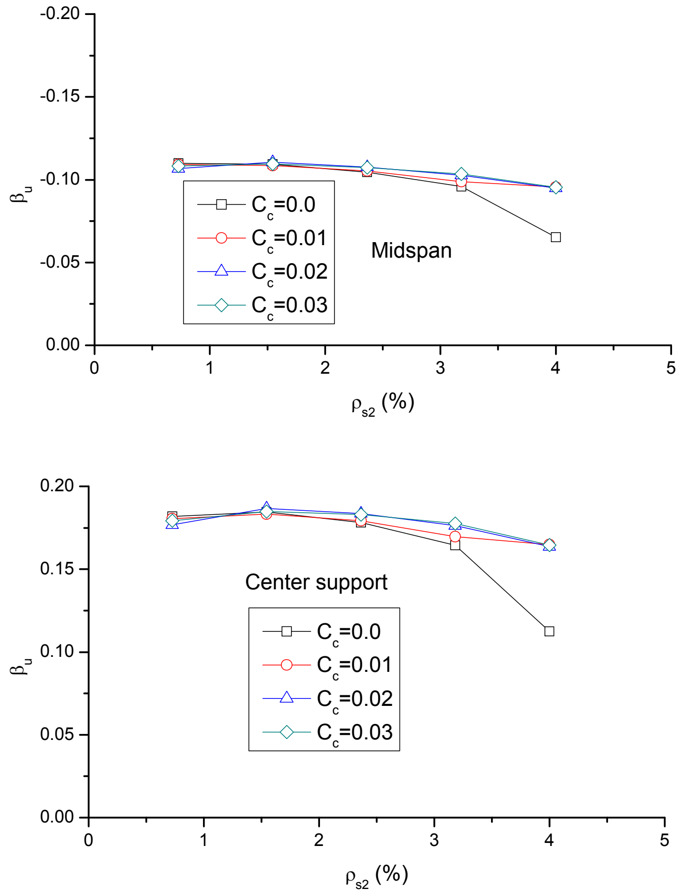

Fig. 11 Variation of the degree of redistribution with steel ratio for different confinement conditions

having sufficient amount of steel due to the stabilization of crack evolution. The higher the amount of steel, the more extensive would be the plateau. The beams with ρ_{s2} of 0.73%, however, do not exhibit such a plateau. This may be explained by the fact of crack concentration appearing in the beams containing a very low tensile steel ratio. After the formation of plastic hinge at the center support (first yielding), the redistribution resumes a quick increase until the formation of plastic hinges at midspan (second yielding). Thereafter, the variation of β is rather limited. The limited increase in redistribution can be attributed to that the stiffness difference between the critical negative and positive moment sections, which is a leading factor influencing the moment redistribution, tends to stabilize after second yielding. Therefore, it may be concluded that the maximum redistribution developed in a two-span continuous reinforced HSC beam is controlled by the second yielding.

Fig. 11 shows the variation of β_u (degree of moment redistribution at ultimate) with the steel ratio for different confinement conditions. It can be observed that, except for unconfined concrete where ρ_{s2} is greater than 3.18%, a higher steel ratio leads to a slight higher (for ρ_{s2} not greater than 1.55%) or lower (for ρ_{s2} greater than 1.55%) value of β_u; and at a given steel ratio, the values of β_u for different confinement conditions are almost identical. For unconfined concrete, the value of β_u

dramatically decreases as ρ_{s2} increases from 3.18% to 4%. As a consequence, at ρ_{s2} of 4%, the value of β_u for unconfined concrete is much lower than that for confined concrete. These observations can be explained by the fact that the redistribution at ultimate is controlled by the formation of plastic hinges at midspan (second yielding) as discussed above. All analyzed beams have yielded at midspan, except for the beam with unconfined concrete and ρ_{s2} of 4%. Based on the above observations, it may be concluded that, for reinforced HSC continuous beams where both the positive and negative plastic hinges have formed at the failure load, the degree of redistribution is nearly independent of the concrete confinement but is slightly influenced by the steel ratio. On the other hand, the flexural ductility is heavily affected by the steel ratio and concrete confinement as presented earlier. Therefore, the influence of steel ratio and confinement on the moment redistribution in reinforced HSC continuous beams is totally different from that on the ductility, although the moment redistribution is considered to be closely linked to the flexural ductility.

5. Comparison with code predictions

Four code recommendations are investigated, namely, EC2 (CEN 2004), BSI (BSI 2007), CSA (CSA 2004) and ACI (ACI Committee 318 2011). The EC2, BSI and CSA equations, where the parameter c_u/d (ratio of the neutral axis depth at the ultimate limit state to the effective depth of a cross section) is adopted to calculate permissible moment redistribution, are represented by Eqs. (8), (9) and (10), respectively.

$$\beta_u \le \lambda - 1.25[0.6 + (0.0014/\varepsilon_u)]c_u/d \tag{8}$$

$$\beta_u(\%) \le 60 - 100c_u/d \tag{9}$$

$$\beta_u(\%) \le 30 - 50c_u/d \tag{10}$$

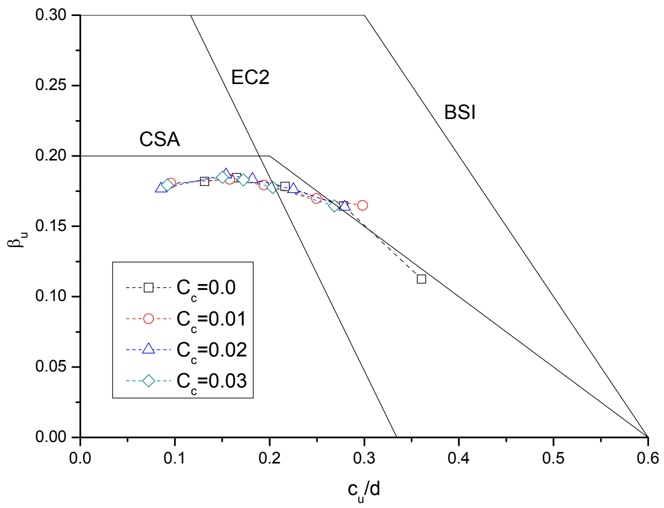

Fig. 12 The β_u-c_u/d relationships according to FEA and various codes

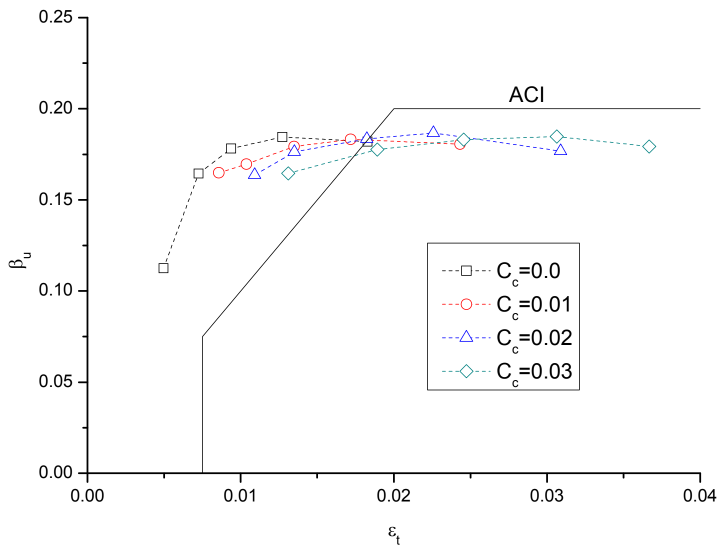

Fig. 13 The β_u-ε_t relationships according to FEA and the ACI code

in which λ=0.46 for HSC. The maximum redistribution is 30% for EC2 and BSI while 20% for CSA.

On the other hand, according to the ACI code, it shall be allowed to decrease factored moments obtained based on the elastic theory by

$$\beta_u(\%) \le 1000\varepsilon_t \tag{11}$$

with a maximum of 20%, where ε_t is the net strain in extreme tension steel at ultimate. The redistribution of moments can be made only when ε_t is not smaller than 0.0075 at the section where the moment is reduced.

Fig. 12 shows the computational β_u-c_u/d relationship at the center support for different confinement conditions. The code curves by EC2, BSI and CSA are also plotted in the graph for comparison. As far as the variation of β_u with the parameter c_u/d is concerned, there is a good consistency for different degrees of confinement according to the FEA results. The β_u value tends to slightly increase with increasing c_u/d up to approximately 0.15. Thereafter the value of β_u gradually decreases as the neutral axis depth increases. It is generally observed that the design codes are able to reflect the tendency of the variation of β_u with the parameter c_u/d. Also, it is seen that the BSI code is unsafe, while the CSA code and EC2 may be nonconservative at a low c_u/d ratio (c_u/d < 0.26 for CSA and 0.2 for EC2). The computational β_u-ε_t relationship at the center support as well as the ACI curve is illustrated in Fig. 13. According to the numerical analysis, the value of β_u increases with increasing ε_t up to approximately 0.01 and then tends to stabilize with continuing increase of ε_t. Generally, the tendency of the variation of β_u with the parameter ε_t can be reflected in the ACI code. However, it would be nonconservative for the ACI code at a high value of ε_t (ε_t > 0.0185).

Fig. 14 illustrates the variation of β_u at the center support with the steel ratio for different confinement conditions according to predictions by various codes. The results produced by FEA

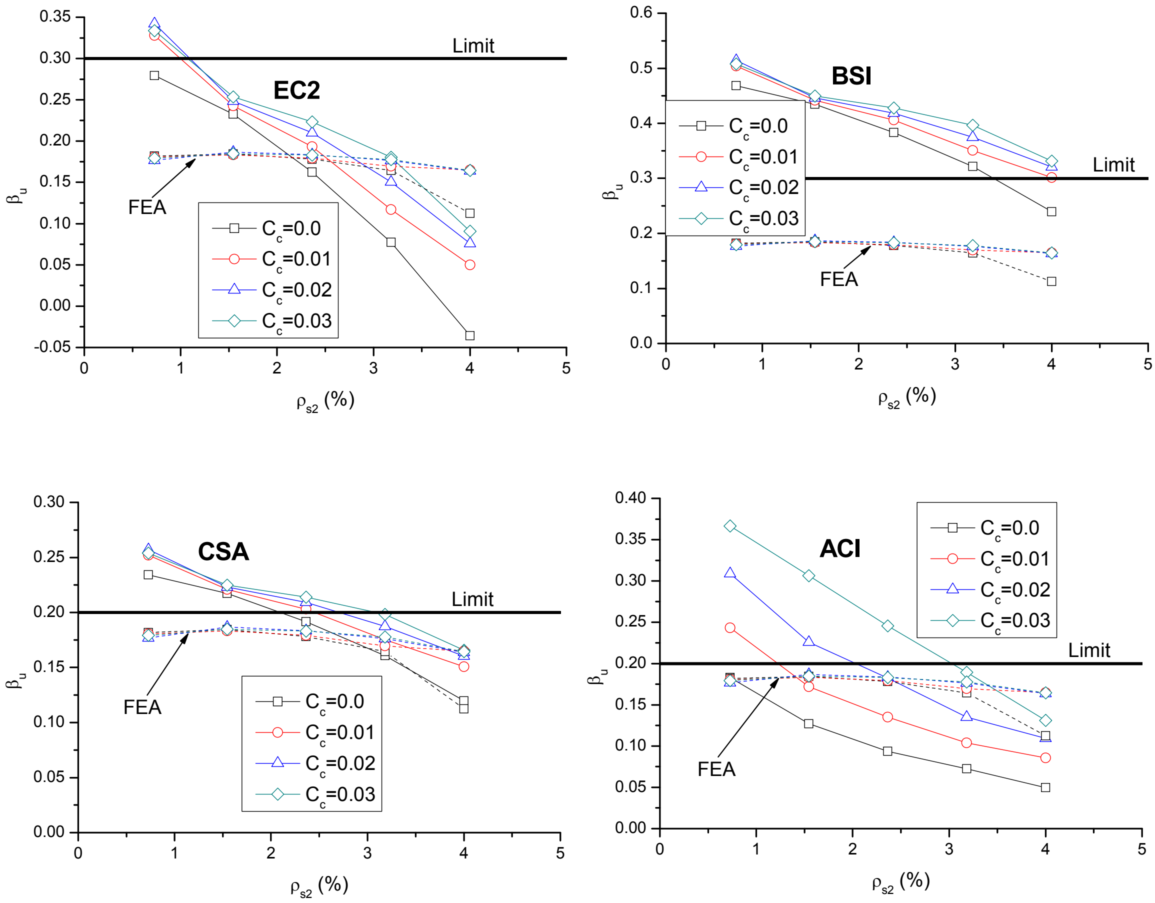

Fig. 14 Comparison of the degrees of redistribution by FEA with code predictions

Table 1 Results in relation to moment redistribution for different confinement conditions and various steel ratios

C_c	ρ_{s2} (%)	c_u/d (%)	ε_t (%)	M_u (kN·m)	M_e (kN·m)	β_u (%) Eq. (8) (EC2)	Eq. (9) (BSI)	Eq. (10) (CSA)	Eq. (11) (ACI)	FEA
0.0	0.73	13.13	1.83	-440.75	-538.75	27.94	46.87	23.43	18.29	18.19
	1.55	16.53	1.27	-837.87	-1027.44	23.28	43.47	21.74	12.71	18.45
	2.36	21.65	0.94	-1228.48	-1494.87	16.23	38.35	19.17	9.37	17.82
	3.18	27.82	0.73	-1605.86	-1921.99	7.75	32.18	16.09	7.26	16.45
	4.0	36.05	0.50	-1947.92	-2194.78	-3.57	23.95	11.98	4.96	11.25
0.01	0.73	9.59	2.43	-447.05	-545.56	32.82	50.41	25.21	24.33	18.06
	1.55	15.80	1.72	-856.79	-1049.03	24.28	44.20	22.10	17.18	18.33
	2.36	19.40	1.35	-1252.22	-1525.83	19.32	40.60	20.30	13.50	17.93
	3.18	24.94	1.04	-1637.24	-1971.67	11.70	35.06	17.53	10.38	16.96
	4.0	29.83	0.86	-1996.23	-2390.27	4.98	30.17	15.08	8.57	16.48

Table 1 Continued

0.02	0.73	8.56	3.09	-463.37	-562.86	34.23	51.44	25.72	30.89	17.68
	1.55	15.39	2.26	-877.05	-1078.34	24.84	44.61	22.31	22.58	18.67
	2.36	18.17	1.82	-1281.11	-1569.12	21.02	41.83	20.92	18.24	18.35
	3.18	22.52	1.35	-1663.16	-2019.18	15.04	37.48	18.74	13.51	17.63
	4.0	27.94	1.09	-2035.19	-2433.62	7.59	32.06	16.03	10.92	16.37
0.03	0.73	9.19	3.67	-474.57	-578.23	33.36	50.81	25.40	36.67	17.93
	1.55	15.02	3.06	-907.37	-1113.08	25.34	44.98	22.49	30.64	18.48
	2.36	17.23	2.45	-1318.64	-1614.08	22.31	42.77	21.39	24.55	18.30
	3.18	20.33	1.89	-1707.12	-2075.87	18.05	39.67	19.84	18.92	17.76
	4.0	26.86	1.31	-2069.19	-2476.61	9.07	33.14	16.57	13.10	16.45

are also included in the graphs for comparative purpose. A summary of the results in relation to moment redistribution at ultimate over the center support for different confinement conditions and various steel ratios is given in Table 1, where M_u is actual ultimate moment. It is seen from Fig. 14 and Table 1 that, according to the predictions by code equations, irrespective of the confinement conditions the value of β_u quickly decreases as the steel ratio increases. However, the FEA indicates that the variation of β_u with increasing steel ratio is slight except for the unconfined concrete at steel ratios greater than 3.18%. Therefore, the code equations cannot well predict the actual trend of the variation of β_u with increasing steel ratio, especially for the confined concrete. Concerning the influence of confinement on the degree of redistribution at ultimate, it can be observed that the EC2, BSI CSA equations can satisfactorily reflect the actual effect but the ACI equation cannot. According to the ACI equation, at a given steel ratio a higher degree of confinement leads to much higher redistribution of moments at ultimate. This phenomenon contradicts with the predictions by FEA which show that the confinement has insignificant influence on the moment redistribution provided that the tensile steel over both the critical negative and positive moment sections has yielded at the failure load as discussed previously. Therefore, the parameter c_u/d (adopted by EC2, BSI and CSA) is better than the parameter ε_t (adopted by ACI) to reflect the effect of confinement on β_u.

6. Conclusions

An investigation has been carried out to examine the effects of concrete confinement as well as steel ratio on the redistribution of moments in two-span continuous reinforced HSC beams. The results of the numerical analysis are consistent with experimental observations regarding the influence of confinement on moment redistribution in HSC beams. The main conclusions drawn are as follows:

• The analysis confirms that the ductility of continuous reinforced HSC beams is highly dependent on the concrete confinement and steel ratio. Although there is a close relationship between flexural ductility and moment redistribution, the influence of concrete confinement and steel ratio on moment redistribution is completely different from that on flexural ductility.

• In a two-span continuous reinforced HSC beam, the maximum redistribution of moments that can be reached is controlled by the second steel yielding. The increase in moment redistribution after second yielding is rather limited.

• Provided that the tensile steel at both the center support and midspan has yielded at failure (this is generally true for practically designed HSC continuous beams), the degree of moment redistribution at ultimate is almost independent of the concrete confinement but is slightly influenced by the steel ratio.

• All the code equations studied (i.e., EC2, BSI, CSA and ACI) fail to accurately reflect the influence of steel ratio on the moment redistribution in reinforced HSC continuous beams, especially when the concrete is confined. The effect of confinement on the moment redistribution is well reflected in the EC2, BSI and CSA equations but it is not reflected in the ACI equation.

Acknowledgments

This research is sponsored by FEDER funds through the program COMPETE (Programa Operacional Factores de Competitividade) and by national funds through FCT (Fundação para a Ciência e a Tecnologia) under the project PEst-C/EME/UI0285/2013. The work presented in this paper has also been supported by FCT under Grant No. SFRH/BPD/66453/2009.

References

ACI Committee 318 (2011), "Building code requirements for structural concrete (ACI 318-11) and commentary", American Concrete Institute, Farmington Hills, MI.

Bai, Z.Z. and Au, F.T.K. (2013), "Flexural ductility design of high-strength concrete columns", *Struct. Des. Tall Spec. Build.*, **22**, 92-115.

Bernardo, L.F.A. and Lopes, S.M.R. (2004), "Neutral axis depth versus flexural ductility in high-strength concrete beams", *J. Struct. Eng.*, **130**(3), 452-459.

BSI (2007), "Structural use of concrete-Part 1: Code of practice for design and construction", BS8110, British Standards Institution, London, UK.

Campione, G., Fossetti, M., Minafò, G. and Papia, M. (2012), "Influence of steel reinforcements on the behavior of compressed high strength R.C. circular columns", *Eng. Struct.*, **34**, 371-382.

Carmo, R.N.F. (2004), "Plastic rotation and moment redistribution in high strength concrete beams", PhD thesis, University of Coimbra, Coimbra, Portugal. (in Portuguese)

Carmo, R.N.F. and Lopes, S.M.R. (2008), "Available plastic rotation in continuous high-strength concrete beams", *Can. J. Civil Eng.*, **35**(10), 1152-1162.

CEB-FIP (1990), "Model code for concrete structures", Euro-International Committee for Concrete-International Federation for Prestressing, Thomas Telford Services Ltd., Lausanne, Switzerland.

CEN (2004), "Eurocode 2 (EC2): Design of concrete structures-Part 1-1: General rules and rules for buildings", EN 1992-1-1, European Committee for Standardization, Brussels, Belgium.

CSA (2004), "Design of concrete structures", A23.3-04, Canadian Standards Association, Mississauga, Ontario, Canada.

Cucchiara, C., Fossetti, M. and Papia, M. (2012), "Steel fibre and transverse reinforcement effects on the behaviour of high strength concrete beams", *Struct. Eng. Mech.*, **42**(4), 551-570.

El-Mogy, M.A.T. (2011), "Behaviour of continuous concrete beams reinforced with FRP bars", PhD Thesis, University of Manitoba, Winnipeg, Canada.

FIB (2012), "Model Code 2010", Bulletins 55 and 56, International Federation for Structural Concrete, Lausanne, Switzerland.

Galano, L. and Vignoli, A. (2008), "Strength and ductility of HSC and SCC slender columns subjected to

short-term eccentric load", *ACI Struct. J.*, **105**(3), 259-269.
Ho, J.C.M., Lam, J.Y.K. and Kwan, A.K.H. (2010), "Effectiveness of adding confinement for ductility improvement of high-strength concrete columns", *Eng. Struct.*, **32**, 714-725.
Hwang, S.K. and Yun, H.D. (2004), "Effects of transverse reinforcement on flexural behaviour of high-strength concrete columns", *Eng. Struct.*, **26**(1), 1-12.
Kassoul, A. and Bougara, A. (2010), "Maximum ratio of longitudinal tensile reinforcement in high strength doubly reinforced concrete beams designed according to Eurocode 8", *Eng. Struct.*, **32**, 3206-3213.
Kodur, V.K.R. and Campbell, T.I. (1999), "Factor governing redistribution of moment in continuous prestressed concrete beams", *Struct. Eng. Mech.*, **8**(2), 119-136.
Kwan, A.K.H., Au, F.T.K. and Chau, S.L. (2004), "Theoretical study on effect of confinement on flexural ductility of normal and high-strength concrete beams", *Mag. Concrete Res.*, **56**(5), 299-309.
Lou, T., Lopes, S.M.R. and Lopes, A.V. (2013), "Flexural response of continuous concrete beams prestressed with external tendons", *J. Bridge Eng.*, **18**(6), 525-537.
Lou, T., Lopes, S.M.R. and Lopes, A.V. (2014a), "Flexure of continuous HSC beams with external CFRP tendons: Effects of fibre elastic modulus and steel ratio", *Compos. Struct.*, **116**, 29-37.
Lou, T., Lopes, S.M.R. and Lopes, A.V. (2014b), "Evaluation of moment redistribution in normal-strength and high-strength reinforced concrete beams", *J. Struct. Eng.*, **140**(10), 04014072.
Lou, T., Lopes, S.M.R. and Lopes, A.V. (2014c), "Factors affecting moment redistribution at ultimate in continuous beams prestressed with external CFRP tendons", *Compos. Part B: Eng.*, **66**, 136-146.
Lou, T., Lopes, S.M.R. and Lopes, A.V. (2014d), "FE modeling of inelastic behavior of reinforced high-strength concrete continuous beams", *Struct. Eng. Mech.*, **49**(3), 373-393.
Moucessian, A. (1986). "Nonlinearity and continuity in prestressed concrete beams", PhD Thesis, Queen's University at Kingston, Kingston, Canada.
Sheikh, S.A., Laine, D. and Cui, C.Y. (2013), "Behavior of normal- and high-strength confined concrete", *ACI Struct. J.*, **110**(6), 989-999.

CC